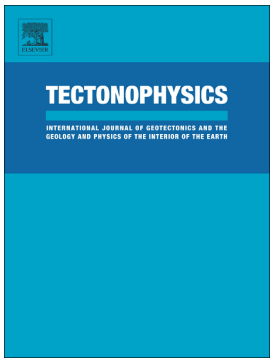

Geometry and late Mesozoic-Cenozoic evolution of the Salar de Atacama Basin (22°30′-24°30′S) in the northern Central Andes: New constraints from geophysical, geochronological and field data

Sebastián Bascuñán, Andrei Maksymowicz, Fernando Martínez, Juan Becerra, César Arriagada, Katja Deckart

PII: S0040-1951(19)30117-9
DOI: https://doi.org/10.1016/j.tecto.2019.04.008
Reference: TECTO 128080

To appear in: *Tectonophysics*

Received date: 31 July 2018
Revised date: 7 March 2019
Accepted date: 7 April 2019

Please cite this article as: S. Bascuñán, A. Maksymowicz, F. Martínez, et al., Geometry and late Mesozoic-Cenozoic evolution of the Salar de Atacama Basin (22°30′-24°30′S) in the northern Central Andes: New constraints from geophysical, geochronological and field data, Tectonophysics, https://doi.org/10.1016/j.tecto.2019.04.008

Geometry and late Mesozoic-Cenozoic evolution of the Salar de Atacama Basin (22°30'-24°30'S) in the northern Central Andes: New constraints from geophysical, geochronological and field data.

Bascuñán, Sebastián[1*]; Maksymowicz, Andrei[2]; Martínez, Fernando[3]; Becerra, Juan[4]; Arriagada, César[1]; Deckart, Katja[1,5].

[1]Departamento de Geología, Facultad de Ciencias Físicas y Matemáticas, Universidad de Chile, Plaza Ercilla 803, Santiago, Chile.

[2]Departamento de Geofísica, Facultad de Ciencias Físicas y Matemáticas, Universidad de Chile, Blanco Encalada 2002, Santiago, Chile.

[3]Departamento de Geología, Universidad Católica del Norte, Angamos 0610, Antofagasta, Chile.

[4]SQM Salar S.A., El Trovador 4285, Las Condes, Santiago, Chile.

[5]Advanced Mining Technology Center, FCFM, Universidad de Chile, Av. Tupper 2007, Santiago, Chile

*Corresponding author

Keywords: Gravimetry, seismic profiles, geochronology, compression, Andes, Salar de Atacama.

Abstract

The late Mesozoic-Cenozoic evolution of the Central Andes of northern Chile consists of a series of events related to changing conditions along the plate margin, leading to different episodes of compression and extension. A long-lasting basin which records these changes corresponds to the Salar de Atacama Basin. Its tectonic history has been blurred by several interpretations of seismic reflection lines and multiple chronostratigraphic correlations between subsurface-surface units. As such, many aspects of its tectonic evolution are still unclear. In this study, we performed an E-W

gravimetric profile across the Barros Arana Syncline and the basin. We analyzed interval velocities obtained from seismic reflection studies and reviewed the profiles closest to the gravity survey. Four U-Pb samples for detrital zircon analysis were obtained from Late Cretaceous-Paleogene units. Geophysical data show a segmentation of physical properties within the basin, with denser units and faster interval velocities around the late Mesozoic-early Cenozoic units, and lighter, slower units in the actual salt pan. The main contrast in physical properties is observed in the evaporitic and fine-grained continental deposits of the San Pedro Formation. Geophysical and geological constraints show that its thickness varies between 800-1200 m, and that it was deformed during later events. The U-Pb data show that the rocks within the Barros Arana Syncline reach well into the Paleogene, and that they were mainly deformed during the late Eocene Incaic Event, where an east-verging thrust system also involving Permo-Triassic units was developed, establishing the actual structural configuration. The late Oligocene-early Miocene units were then deposited in a post-orogenic setting, with minor compression. A stronger phase around the late Miocene reactivated previous structures and folded these deposits. This continuous, compressive history of the basin, which is mostly a result of the Incaic Event, is in agreement with the regional evolution of the Central Andes.

1.-Introduction

The Central Andes of northern Chile (Figure 1;Gansser, 1973; Ramos, 2010, 2009) constitute a prime interest zone for the understanding of the building of the Andean Cordillera. Its evolution has been marked by different stages of arc-parallel extension and compression related to subduction dynamics, of which some have been identified independently along different areas of the Central Andes (e.g., Charrier et al., 2009, 2007; Cobbold et al., 2007; Kay et al., 2005; Martínez et al., 2013, 2012; Megard, 1984; Noblet et al., 1996; Ramos, 2010, 2009; Sempere, 1995). The understanding of these events and their relation to one another is crucial to unraveling the tectonic history of the South American margin.

A key location for studying the evolution and configuration of the Andean Orogen is the Salar de Atacama Basin, in the Preandean Depression (Figure 1). The basin presents a remarkable exposition of Paleozoic to Cenozoic outcrops recording much of the geological history of northern Chile (Figures 2 & 3), along with multiple seismic lines and a 5425-m deep well (Toconao-1) obtained by the Empresa Nacional del Petroleo (ENAP), which has led to many studies regarding its structure, geochronology and stratigraphy (e.g., Arriagada et al., 2006a; Bascuñán et al., 2016; Brüggen, 1950, 1942, 1934; Charrier and Muñoz, 1994; Charrier and Reutter, 1994, 1990; Dingman, 1967, 1963; Flint et al., 1993; Hartley et al., 1992a, 1988, Jordan et al., 2007, 2002; Macellari et al., 1991; Mpodozis et al., 2005; Naranjo et al., 1994; Pananont et al., 2004; Reutter et al., 2006; Rubilar et al., 2017) . However, in spite of the growing amount of knowledge obtained over the last 30 years, many questions remain regarding the tectonic conditions during the late Mesozoic-Cenozoic, and the transition between different compressive deformation events, such as the Peruvian Phase (around 100-70 Ma; Cobbold et al., 2007; Fildani et al., 2003; Jaillard, 1993, 1992; Jaimes and de Freitas, 2006; Steinmann, 1929), the KT Event (around 65 Ma; Cornejo et al., 2003, 1993; Somoza et al., 2012) and the Incaic Event (ca. 45-32 Ma; Arriagada et al., 2008; Bosio et al., 2009; Charrier et al., 2009; Del Papa et al., 2013; Hongn et al., 2007; Montero-López et al., 2018; O'Driscoll et al., 2012; Steinmann, 1929). Some authors have argued for an evolution under mostly compressive conditions since ca. 90 Ma (Arriagada et al., 2006a), while others suggest an important post-orogenic extensional event for the late Oligocene-early Miocene interval, which provoked localized mechanical subsidence of the basin (Figure 4; Flint et al., 1993; Jordan et al., 2007; Pananont et al., 2004; Rubilar et al., 2017). Part of this discrepancy arises from opposite interpretations of seismic lines, the complex stratigraphy of the Toconao-1 well, and the multiple chronostratigraphic proposals for the units cropping out in the El Bordo Escarpment (Figure 2). The lack of additional independent constraints has been thus detrimental to the final evaluation of the seismic lines, the understanding of basin geometry, and to the establishment of a clear regional evolution.

In this work, we performed a gravimetry survey along an E-W profile involving the actual salt pan and the late Mesozoic-Cenozoic synorogenic deposits, together with an analysis of interval velocities and a reexamination of previous seismic reflection profiles (Figure 2). We also analyze four new U/Pb detrital zircon samples in order to provide a more concise time frame for the structural evolution of the basin. This combination of data allows us to clarify the tectonic setting since the Late Cretaceous, and to propose a congruent model involving the events found both in the basin and around the northern Central Andes.

2.-Geological Setting

The Salar de Atacama Basin is an intramontane basin located between 22°30'-24°30'S, west of the magmatic arc and east of the Cordillera de Domeyko (Figures 1 & 2), which consists of Paleozoic to Mesozoic rocks bounded by doubly verging, high-angle reverse faults (Amilibia et al., 2008; Breitkreuz and Van Schmus, 1996). The Cordillera de Domeyko is interpreted to have been a prominent part of the Andean orogenic front between the Late Cretaceous and the Eocene (Arriagada et al., 2006a; Bascuñán et al., 2016; Charrier et al., 2009; Maksaev and Zentilli, 1999). An abrupt topographic change towards the east of this range (El Bordo Escarpment) delineates the border between the Salar de Atacama Basin and the Cordillera de Domeyko (Figure 2). The topographic relief in this area can reach up to 900 m, where mainly Paleozoic to Tertiary rocks are exposed (Arriagada, 1999; Arriagada et al., 2006a; Basso and Mpodozis, 2012; Hammerschmidt et al., 1992). The southern end of the basin is composed of igneous and sedimentary rocks of Ordovician-Carboniferous age exposed along the Cordón de Lila (Coira et al., 2009; Niemeyer, 2013, 1989; Zimmermann et al., 2009). Northwards, the basin abuts against Pliocene-Miocene ignimbrites and other volcanic deposits, which are also found east, as the basin slope gradually rises

towards the current magmatic arc (Becerra et al., 2014; Henríquez et al., 2014; Marinovic and Lahsen, 1984; Ramírez and Gardeweg, 1982).

Several distinct structural features can be recognized within the basin. From west to east, these are the Barros Arana Syncline, the Llano de la Paciencia, the Cordillera de la Sal and the current saltpan (Figure 2). The Barros Arana Syncline is an 80-km long and 16-km wide, NE-SW-oriented syncline, comprised of Upper Cretaceous-Paleogene synorogenic volcanic and sedimentary rocks belonging to the Tonel, Purilactis and Barros Arana Formations (Figures 2, 3 & 4; Arriagada, 1999; Arriagada et al., 2006a; Bascuñán et al., 2016; Charrier and Reutter, 1994; Hartley et al., 1992a, 1988, Mpodozis et al., 2005, 1999; Reutter et al., 2006). An unconformity separates these rocks from the Oligocene-Miocene Tambores Formation, and other Miocene to Pliocene clastic deposits (Henríquez et al., 2014; Marinovic and Lahsen, 1984).

Recent provenance and geochronological studies have shown that the constituents of these sediments came from an uplifted source to the west, whose location changed progressively from the Coastal Cordillera (Figure 1) to the Cordillera de Domeyko, between 107 Ma-73 Ma, associated with the eastward migration of the Late Cretaceous contractional deformation front in this part of northern Chile (Bascuñán et al., 2016). The migration of the foreland has been associated with the mid-Cretaceous Peruvian Tectonic Phase (Steinmann, 1929), a compressional event which has been recorded in different parts of the South American margin, albeit with slightly different timings between 100-75 Ma (Cobbold and Rossello, 2003; Gianni et al., 2015; Jaillard, 1993, 1992; Jaimes and de Freitas, 2006; Megard, 1984; Merino et al., 2013; Tunik et al., 2010).

The Llano de la Paciencia lies east of the El Bordo Escarpment/Barros Arana Syncline, and west of the Cordillera de la Sal (Figure 2). It is an 80-km long and 8-km wide sub-basin filled mostly by Quaternary alluvial deposits (Jolley et al., 1990; Marinovic and Lahsen, 1984; Mpodozis et al., 2005). A relevant increase eastward in the slope of the salar marks the beginning of the Cordillera

de la Sal, an elongated, SSW-NNE-oriented thin-skin fold belt with a topographic relief of 200 m compared with the basin floor (2300 m a.s.l) (Becerra et al., 2014; Wilkes and Görler, 1994). It is comprised of Oligocene-Miocene evaporites and terrigenous deposits belonging to the San Pedro Formation (part of the Paciencia Group *sensu* Flint, 1985; see Table 1 for ages), and Pliocene to recent evaporites, lacustrine and fluvial deposits (Vilama and Campamento Fms; Arriagada et al., 2006a; Flint et al., 1993; Jordan et al., 2002; Rubilar et al., 2017). The deposits of the San Pedro Formation show a maximum estimated thickness of 3000-3200 m in some parts of the Cordillera de la Sal (Figure 5), and its origin is related to the erosion of the units exposed along the El Bordo Escarpment (Figures 3 & 4; Arriagada et al., 2006a; Becerra et al., 2014; Henríquez et al., 2014; Jordan et al., 2007; Mpodozis et al., 2000; Pananont et al., 2004; Wilkes and Görler, 1994). Regarding the modern-day saltpan, its infill has been identified as alluvial and evaporitic deposits of Quaternary and older age, overlying a complexly deformed substrate (Arriagada et al., 2006a; Flint et al., 1989; Jordan et al., 2007; Macellari et al., 1991; Muñoz et al., 2002; Pananont et al., 2004; Reutter et al., 2006).

A variety of geophysical studies have been carried out both within and around the Salar de Atacama Basin, mainly focusing on its mid to upper crustal structure and composition. These include seismic reflection profiles carried out by ENAP (Empresa Nacional del Petróleo), gravity surveys (Götze et al., 1994; Götze and Krause, 2002) and seismic studies (Schmitz et al., 1999; Schurr and Rietbrock, 2004; Yuan et al., 2002). These studies show that a distinct gravity high can be found beneath the basin, which would correspond to a high-density body found 10 to 38 km beneath the saltpan, possibly consisting in a mix of gneisses and metabasites with moderate Vp/Vs ratios, rheologically strong and thermally cold. Also, the Moho depth (ca. 67 km) seems to be anomalously high for the current altitude of the basin, which, together with previous data, suggests that the block is mechanically coupled to the Nazca plate, thus apparently explaining local elevation (Yuan et al., 2002).

The interpretations of the subsurface of the basin have varied importantly over the last 25 years, showing at times contrasting results. Flint et al. (1993) argued for extensional (and later strike-slip) conditions dominating most of the basin history from the Permo-Triassic up to the Miocene, based on their analysis of five sequences. Muñoz et al. (2002) analyzed the Toconao-1 well results and the seismic line that intersects it, and obtained six (seven including the basement) stratigraphic sequences ranging from the mid-Cretaceous (Cenomanian-Maastrichtian) to the Holocene. They concluded that the basin had experienced moderate extension during the Late Cretaceous, followed by strong inversion during the early Paleocene, and basement-involved tectonics during the Eocene. This deformation would have later transferred in sequence to younger layers, thus establishing a mainly compressive history for the basin. This tectonic frame was then brought into question by Pananont et al. (2004), who reinterpreted the seismic section associated with the well, obtaining six sequences which were then extended northwards in order to interpret some of the northernmost seismic lines (Figures 2 & 4a). They also used the results from Jordan et al. (2002), who analyzed some of the southernmost lines and studied the shallow evaporitic units (down to 900 m in depth approximately) of the salt pan. Under their new proposal, the mid-Cretaceous to Paleocene-Eocene sequences would represent deposition under mostly compressive conditions, with the latter representing the deposits associated with the Incaic Orogeny. Afterwards, east-west extension, combined with some degree of transtension, would have generated a large normal fault, which led to the deposition of Oligo-Miocene deposits (Figure 4a). A similar view was held by Jordan et al. (2007), who reviewed most of the seismic sections and elaborated thickness maps for the different sequences. Both Pananont et al. (2004) and Jordan et al. (2007) argue for a return to compressive conditions at the end of the early Miocene. On the other hand, Arriagada et al. (2006a), based on their interpretation of the seismic sections and the Toconao-1 well, along with multiple field observations, suggest the presence of at least six sequences within the basin, which are associated with the outcrops along the El Bordo Escarpment, following the chronostratigraphy developed by

Mpodozis et al. (2005). The Salar de Atacama Basin would mostly record compressive conditions since 90 Ma, with no evidence for large extensional processes (Figure 4b).

More recently, Rubilar et al. (2017) performed a structural reconstruction of several cross-sections perpendicular to the Cordillera de la Sal, which were based on their interpretation of seismic sections belonging mostly to the central and southern parts of the basin. Their results show the wide presence of inversion tectonics during the Neogene, which would have been facilitated by the presence of Oligocene synextensional evaporites. These evaporites act as a detachment level and show a south-to-north deepening; these levels are associated with the extensional episode posited by some of the authors mentioned above.

3.-Methodology

3.1.-Seismic reflection profiles

A subset of the seismic reflection profiles provided by ENAP has been used in this study (Figure 2), covering roughly the northernmost parts of the basin, comprising around 77 km of sections acquired with a Vibroseis source. These lines correspond to 1F008-1F008A (Figure 6) and 1F010-1F010A (Figure 7), some of which have been previously studied with varying interpretations (Figure 4). The seismic lines, whose static corrections followed a sloping datum, were adjusted to the SRTM DEM topography by modifying trace position. The highest value becomes fixed at 0 s TWT, and each trace at a lower altitude is shifted in the time domain using a replacement velocity of 3500 m/s. This process was performed with Seismic Unix and Python tools. The seismic profiles were depth-converted using Move 2017.1. by Midland Valley Ltd., following equation (2), which is itself a derivation of a linear equation relating instantaneous velocity to depth (e.g., Al-Chalabi and Rosenkranz, 2002)

(2) $Z\ (m) = V_0{*}(e^{kt} - 1)/k$

Where Z is the thickness of the top layer in meters, V_0 is the velocity at the top of the layer in m/s, k is the rate at which velocity changes with depth and t is the one-way travel time for layer thickness, in seconds.

Assuming a fixed velocity of V_0= 3500 m/s (within the velocity range from the CDP velocity data, see below), k equals 0, and accounting for two-way travel time, equation (2) becomes:

(3) $Z(m) = V_0 t/2$

The seismic profiles were then interpreted following standard seismic reflection techniques, such as identifying tectonic and/or stratigraphic reflector truncations, grouping the sequences according to the nature of their reflectors (continuity, spacing and amplitude), and identifying seismic surfaces and sequence boundaries (Catuneanu et al., 2011; Cross and Lessenger, 1988). The grouping of the different sequences follows closely those proposed by earlier authors (Arriagada et al., 2006a; Jordan et al., 2007; Pananont et al., 2004), and the geological maps by Becerra et al. (2014) and Henríquez et al. (2014).

3.2.-CDP Velocity

Another way to estimate the depth at which physical properties change in the seismic sections is by analyzing the Common Depth Point (CDP) interval velocity, generated through NMO processing. These were found in some of the paper versions of the seismic lines provided by ENAP (seismic lines 1H100, 1H104, 1H107, 1H108, 1H116, 1H120, 1H121, 1H124, 1H125, 1H128, 1H130, 1H134, 1H135, 1H138 AND 1H143), showing root mean square 1D velocities at certain TWT depths for points spaced on horizontal axis between 2-2.5 km. This data was digitized and converted to interval velocities following the relation described by Dix (1955):

(1)

$$V_{int} = [\frac{t_2 * {V_{RMS2}}^2 - t_1 * {V_{RMS1}}^2}{t_2 - t_1}]^{1/2}$$

The resulting values were lineally interpolated and gridded using a combination of GMT and Python, thus producing different map view velocity slices spaced 250 m a. s. l. (Figure 8). For simplicity, and to start with an elevation common to all lines, the slices started at 2000 m a.s.l., although some sections, particularly those to the west, reach higher altitudes (around 3300 m a.s.l.). A velocity cross-section following the trace of the gravimetric survey was also obtained, together with a combination of lines 1H100 and 1H120 (Figure 9).

3.3.-Gravity data

An E-W gravity profile was carried out within the Salar de Atacama Basin in order to test current structural models regarding its internal architecture (Figure 4). The profile consists of 29 stations, spaced every 1 km (Figure 2). Its strike was semi orthogonal to regional structures such as the Cordillera de la Sal and the Barros Arana Syncline. The objective of the profile was to check and identify any matches between the much-discussed seismic reflection profiles and the gravity response of the different bodies suspected to lie beneath the surface of the actual basin and along its edges. Measurement were taken both on- and off-road, trying to match as closely as possible the surficial traces of the seismic profiles taken during the 1980's. A CG-3 Scintrex Autograv gravity meter, with a 0.005 mGal resolution, was used for all measurements. Coordinates and elevations were acquired with a Topcon-Hiper V D-GPS system. Gravity reduction was done according to standard procedures, such as those described by Blakely (1996). These involve Earth tide correction following the algorithm of Longman (1959), correcting for instrumental drift by performing a time linear interpolation between the daily measurements taken at the gravity base station (0.02-0.2 mGal h^{-1}), removing the normal gravity trend associated with the WGS84 ellipsoid, and applying both free-air and simple Bouguer anomaly corrections with the D-GPS elevation and a background density of 2.67 g/cm^{-3}. Afterwards, the complete Bouguer anomaly was obtained by performing a

terrain correction using a 50x50 km, high-resolution (92x92 m) SRTM digital elevation model (DEM). The data was modeled using ModelVision 13.0 (Figure 10). The measurements can be found in Supplementary Material A.

3.4.-U-Pb Detrital Zircon Geochronology

Another useful tool to understand the geological evolution of a given area, particularly those with few igneous outcrops, corresponds to U-Pb detrital zircon geochronology. Although previous studies have aided in establishing the timeframe of the tectonic evolution of the basin (Bascuñán et al., 2016; Mpodozis et al., 2005), four additional samples belonging to the Purilactis Formation were analyzed (Figure 2 & 5d), in order to evaluate and enhance previous interpretations. The samples correspond to medium- to coarse-grained sandstones belonging to the Pajarito Member (SP3-92), the Vizcachita Member (SP3-86, SP3-84), and the Seilao Member (SP3-85) (Figure 11). Table 1 summarizes the ages of the data presented here and other relevant ages found both within the study area and in neighboring areas around Cordillera de Domeyko, compiled from several sources (Bascuñán et al., 2016; Basso and Mpodozis, 2012; Becerra et al., 2014; de Silva, 1989; Flint et al., 1989; Gardeweg et al., 1994; Hammerschmidt et al., 1992; Henríquez et al., 2014; Marinovic and Lahsen, 1984; Mpodozis et al., 2000, 2005; Naranjo et al., 1994; Ramírez and Gardeweg, 1982; Reiners et al., 2015; Solari et al., 2017; Travisany, 1978).

The samples were processed at the Sample Preparation Laboratory of the Geology Department of the Universidad de Chile, using Gemeni Table, Frantz magnetic separator and heavy liquid procedures. The zircons were separated manually operating a binocular microscope and were then sent to the Laboratorio de Estudios Isotópicos (LEI) of the Geoscience Center of the Universidad Nacional Autónoma de México (UNAM). Around 100 random grains were analyzed with a *Resonetics Resolution M50* 193 nm laser *Excimer* connected to a *Thermo Xii Series Quadrupole Mass Spectrometer*, utilizing a 23 μm laser diameter for ablation. Additional technical details are

described in Solari et al. (2010). All unit ages and designations follow those of the International Stratigraphic Chart (Cohen et al., 2013).

The best age for each zircon was defined using the same criteria as in Bascuñán et al. (2016), and sample age was calculated using *Isoplot v.3.7.* (Ludwig, 2008), obtaining averages for the youngest populations with more than three zircons. Relevant peaks and populations were also analyzed using the spreadsheet Age Pick developed by the LaserChron Center at the University of Arizona. The resulting data tables can be found in Supplementary Material B.

4.-Results

4.1.-Seismic profiles and main structural components

The interpretation of the seismic sections follows some of the basic observations made from previous works, such as those of Pananont et al. (2004), Arriagada et al. (2006a) and Jordan et al. (2007). The geometries and limits of the different sequences were compared and evaluated, observing a general conformity among the authors in the area of the Barros Arana Syncline (Figures 4 & 6). The areas to the east show some divergences, particularly regarding the age of the sequences, which are presented below. Six major sequences were interpreted and correlated with the rocks cropping out around the edges of the Salar de Atacama Basin and its interior (Figure 2). The interpretations are presented in Figures 6 & 7.

Sections F008 and F08A, which are nearly perpendicular to the strike of the Barros Arana Syncline (Figure 2 & 6), show clearly the geometry of this structure, which corresponds to an asymmetric, east-verging syncline, mainly involving Upper Cretaceous and Paleocene synorogenic deposits of

the Purilactis Group (K-Pg). Its limbs loose lateral continuity, and are cut by shallow, high-amplitude reflectors. These have been associated with east- and west- verging reverse faults, some of which can be seen on the surface (Figure 2). The upper section of the fold is unconformably covered by slightly folded, shallow seismic reflectors related to the Oligocene-Miocene deposits of the Tambores Formation (TAM) (Figures 2 & 6). West of the syncline, a series of chaotic reflection patterns have been correlated to Triassic volcano-sedimentary rocks, which have been considered part of the basement of the basin (Tuina Fm, Tr; Henríquez et al., 2014; Narea et al., 2015; Raczynski, 1963). Based on this seismic and structural relation, a basement wedge associated with an east-verging thrust ramp is interpreted to lie underneath the Barros Arana Syncline. This structural style is commonly created from the movement of a basement block detached along the contact between basement and cover rocks. Underlying this zone, some of the most relevant folded seismic reflectors have been identified as part of an east-verging, basement-involved fold, related to east-verging reverse faults. These faults also detach part of the syncline, placing its eastern flank on top of units higher in the stratigraphic column.

East of the Barros Arana Syncline, in the Llano de la Paciencia area, a series of high-amplitude seismic reflectors associated with the Oligocene-Miocene San Pedro Formation (SPF) have been identified (Arriagada et al., 2006a; Becerra et al., 2014; Henríquez et al., 2014; Pananont et al., 2004). These are frequently folded, and show some geometries related to growth strata and wedge shapes similar to those reported for synorogenic deposits. Laterally, these are cut by west- and east-verging, subsidiary thin-skinned thrust faults (Figures 6 & 7). These Cenozoic units show more deformation with closer proximity to the Cordillera de la Sal, and an increase in dip downwards. On the other hand, the Oligo-Miocene units unconformably overlie rocks with low-amplitude, discontinuous reflectors, interpreted here to be part of the same rocks that comprise the Barros Arana Syncline (K-Pg).

The easternmost part of Figure 6 overlaps with sections F010 and F010A (Figure 7), particularly the area between the Llano de la Paciencia and the Cordillera la Sal, although their traces are located 9.5 km to the south (Figure 2). These seismic profile sections clearly show an abrupt angular unconformity between the sub horizontal to east-dipping Oligo-Miocene (SPF) and Late Cretaceous-Paleogene (K-Pg) units and the west-dipping Triassic (Tr?) units beneath them. Here, the Cordillera de la Sal appears as a doubly verging, reverse-fault bound, nearly symmetrical structure (Figure 2). This fault is associated with other deep, high-amplitude reflectors, forming part of an east-verging fault system, in continuation with the structural style seen in the previous sections. East of the Cordillera de la Sal, the Oligo-Miocene units (SPF), which usually display continuous and relatively high-amplitude reflectors, are seen forming broad folds which become tighter closer to the eastern border of the saltpan. The variations in SPF strata thickness follow closely the deformation of the previous strata.

The first-order structural style along these seismic profiles is represented by a set of east-verging reverse faults that appear to affect the basement of the basin. The hanging wall of these faults are composed of asymmetrical anticlines, and the footwall shows footwall syncline folds (Figures 6 & 7). Although the quality of the seismic sections is relatively poor below 1000 m a.s.l., several high-amplitude reflectors delineate a west-dipping surface, which is interpreted as the top of the Triassic-Mesozoic (?) units, based partly on previous interpretations (Figure 4) and the presence of units with a similar age and structural disposition southeast of the study area (Becerra et al., 2014; Niemeyer, 2013). Under the central part, some small-scale features resembling growth strata are also preserved in this surface, which can only be loosely assigned to the Early Cretaceous-Triassic (?) interval. These usually show some variation of thickness, and appear to be accumulated at the hanging wall block of previous normal faults (Figure 7). These units are asymmetrically folded, and have structural geometries associated with tectonic inversion, suggesting thus that previous normal faults were partially reactivated.

The western end of the surface limiting the Triassic and Cretaceous (Tr? K?) sequences is folded into a syncline, which also encompasses some of the units above it (Figure 7). The decrease in dip upwards also highlights the presence of an unconformity between the SPF and older units (Pg, K?), both of which are affected by more recent, reverse faulting. The units between the SPF and the west-dipping reflector show a progressive decrease in thickness eastwards, from around 2000 m in the center of the seismic section (near the syncline axis) to around 1000 m near the eastern limit. These rocks are assigned to the Late Cretaceous-Paleogene interval, based on previous studies (Figure 4) and regional geology (Figure 2).

4.2.-Velocity analysis

The interpolation of the 1D CDP velocity data (Figures 8 & 9) yields relevant data that serves as an independent constraint for the density and structural modeling. Figure 8 shows the velocity map at different altitudes, highlighting the general decrease in velocity from west to east, which is generally more pronounced between 2000-1250 m a.s.l. There are overall high velocity values (3800 m/s and higher) around the western Barros Arana Syncline and close to the Triassic outcrops (Figure 2), which decrease steadily towards its eastern border and the Llano de la Paciencia. The area east of the syncline axis shows lower velocities than its western counterpart, and the pattern becomes more complex with increasing depth. The slices between 1750-1250 m a.s.l. reveal that the area can be separated into several domains, with an overall low velocity zone underneath the Llano de la Paciencia and the western border of the Cordillera de la Sal (with velocities increasing in depth from 2600 m/s to 3300 m/s), another narrow area with higher average velocities underneath the Cordillera de la Sal (starting from 2900 m/s and increasing more rapidly with depth), and another low-velocity area towards the east (velocities around 2600 m/s, shifting rapidly to 3400-3500 m/s between 1250-1500 m a.s.l.). Deeper slices (1000 m a.s.l. and below) show a similar

pattern, with higher velocities below the Cordillera de la Sal area. Another trend seen in deeper slices is a relative increase in velocity north of the gravimetric profile (red dots in Figures 2 & 8), between the Cordillera de la Sal and the Barros Arana Syncline, with velocity values over 4000 m/s, much faster than both the Cordillera de la Sal and the low-velocity domains.

The velocity cross-section illustrates the features discussed above, but presents a clearer view of the data underlying the gravimetric section (Figure 9a). The high-velocity zone, corresponding to Triassic-Cretaceous units is clearly visible, showing a steady decrease in velocity towards the Llano de la Paciencia. This area displays velocities around 3200-3800 m/s, between 350-1150 m a.s.l. This effectively accounts for lower velocities in this area in comparison to its immediate surroundings, related to the low velocities seen in map view. An abrupt change in velocity is recorded in the units east of the Cordillera de la Sal, where a nearly flat surface at ca. 1600 m a.s.l. separates units with velocities below 2800 m/s above the surface, and units with velocities over 3600 m/s beneath it. This "flat" surface displays some asperities, which may be related to the small-scale folds and structures seen in seismic section F10A (Figure 7), and the intense deformation seen in the Cordillera de la Sal. Figure 9b shows the transition from the Tuina Area to the northern Cordillera de la Sal (Figure 2). A prevalence of high velocities around the Tuina-Barros Arana Syncline is also noticeable, with a slight drop in velocity and a "V"-shape geometry for the velocity in the latter part. The area shows a large number of artifacts below 2700 m a.s.l., and abrupt lateral changes in velocity, which become smoother eastwards. East of the syncline, the velocity bands between 2800-4000 m/s adopt a nearly parallel disposition, mimicking the topographic drop eastwards (from 3300 to 2600 m a.s.l.). This 'subparallel' trend is visible up to 4400 m/s, above which the data is more irregular.

4.3.-Gravity Survey and Density Structure

The density modeling was carried out using several constraints to define the geometries of the modeled bodies; a primary source of information was the geological maps by Becerra et al. (2014) and Henríquez et al. (2014). It was assumed that long-wavelength gravity anomalies were a response to density contrasts between the upper Mesozoic-Cenozoic outcrops and the basement, defined as older units belonging especially to the Triassic (such as the Tuina Fm., Figure 2). The latter are found cropping out at the western edge of the profile, thus allowing to define one of the endpoints of the regional gravity trend.

Since the only basement outcrops at the eastern border of the Salar de Atacama are found ca. 38 km south of the eastern end of the profile, it was necessary to use the velocity data (Figure 8 & 9), and the interpretations of the seismic sections (Figures 6 & 7) to constrain the gravity trend. In this way the chosen regional trend is in agreement with more than one independent set of data. More importantly, the overall geometry of the modeled bodies does not undergo significant changes with slight variations of this fix. The dataset mentioned above was also crucial in understanding subsurface structural styles, and both the folding and faulting variations along the section. The bodies were modeled as contrasts relative to a background of density 0 gr/cc^3, represented by the pre-Jurassic formations (Figures 2 & 3). The contrasts for the sedimentary units were chosen after several iterations of the modeling, following the shape of the bodies seen in the seismic sections, the velocity data and the regional geology (see Table 2).

Figure 10 shows the complete Bouguer Anomaly, with multiple short-wavelength deviations from the regional tendency. Following both the seismic sections and the velocity data (Figures 6, 7, 8 & 9), the gravity highs have been linked to the presence near the surface of Triassic rocks and/or structural highs; conversely, the gravity lows have been interpreted as depocenters involving Cretaceous to Paleogene, coarse continental deposits, Oligocene-Miocene evaporites associated with fine-grained clastics, and the Pliocene to recent cover of the saltpan. From west to east, the first gravity low is associated with exposed, folded rocks belonging to the Purilactis and Barros

Arana Formations, which comprise the Barros Arana Syncline (Figure 2). The gravity model shows this structure, though it also requires that some of its lower members be present underneath the basement towards the west. The best fit to the data requires an average density of -0.21 g/cm^3 for the units of the Barros Arana Syncline. It is relevant to note that the hinge of the Barros Arana Syncline does not coincide with the minimum of the local low gravity anomaly observed in the zone (Figure 6), which requires the inclusion of a body with the same density associated to the syncline to the west, and the modeling of thin surficial gravels (-0.47 g/cm^3) belonging to recent deposits and the southern fringes of the outcrops belonging to the Oligocene-Miocene Tambores Formation, which have a reduced thickness in this area (Figures 2 & 6).

Immediately east of the syncline, the following low gravity anomaly shows an east-dipping gradient forming a scoop-shaped geometry (Figure 10). The gravity high separating both lows has been interpreted as a result of the proximity to the surface of basement rocks, which are not seen cropping out (Figures 2, 6 & 7). This area involves the transition from the El Bordo Escarpment-Barros Arana Syncline towards the Llano de la Paciencia-Cordillera de la Sal, with a continuous drop in topography interrupted by a sudden raise in surface topography (up to 200 m). Here, the units observed at the surface involve mainly a recent cover of gravels, which are found unconformably overlying folded deposits belonging to Oligocene-Miocene units towards the east (Figure 5a, b, c). The wedge-shaped geometries seen in Figure 7 are linked to the San Pedro Formation, showing a much lower density than its surrounding counterparts (-0.68 g/cm^3), and some units of the Late Cretaceous-Paleogene. The eastern side of this gravity anomaly roughly coincides at the surface with the eastern limit of the reverse fault-bound Cordillera de la Sal (Figures 2 & 7). It is worth mentioning that the depth of the San Pedro Formation in the profile is deeper than seen in Figure 7, owing to the increase in depth of this limit northwards (around 1200-1300 m in Figure 6). For simplicity, the deposits of the Vilama Formation have been included

within the Oligocene-Miocene deposits for the gravimetric modeling, owing to their reduced thickness in the area (Figure 2; Blanco et al., 2000; Henríquez et al., 2014).

The area east of the Cordillera de la Sal shows both a progressive increase in topography towards the Western Cordillera, and a relatively flat, east-dipping gravity signal (Figure 10). The area presents a recent cover involving gravels and recent evaporites, along with Pliocene ignimbrites towards the east (Figure 2). The density used to model the latter is -0.87 g/cm^3, which is within the range used for modelling similar ignimbrites in the Pacana Caldera, east of the study area (Delgado and Pavez, 2015). This "flat" gravity signal follows both the reflectors seen in the seismic sections (Figure 7) and a prominent change in velocity (Figure 9), separating the evaporitic and fine-grained clastic deposits from the older, denser Cretaceous to Paleogene units. The units show a progressive tapering towards the east, and the basement in the area adopts a west-dipping disposition, as seen in outcrops along the southeastern border of the basin (Figure 7; Becerra et al., 2014).

4.4.-Maximum depositional ages and relevant populations

Sample SP3-85 (Seilao Member, Purilactis Fm.)

The maximum depositional age obtained for the sample belonging to the Seilao Member is 69.1±1.0 Ma (Figure 11a). The major populations are clustered around 294 Ma (n = 24, Permo-Carboniferous), followed by Upper Cretaceous populations (n = 11 and 10 at 70 and 88 Ma, respectively). Other sizeable populations occur between 93-96 Ma (n = 17, mid-Cretaceous), between 78 and 82 (n =9, Late Cretaceous) and at 142 Ma (n = 6, Early Cretaceous). The major relative probability peaks are found at 70 (Maastrichtian) and 294 Ma (Sakmarian), followed by peaks at 88 and 142 Ma (Coniacian and Berriasian, respectively).

Sample SP3-86 (Vizcachita Member, Purilactis Fm.)

The first of two samples of the Vizcachita Member (Figure 11b), obtained close to the contact with the Seilao Member, has a maximum depositional age of 66.8±0.7 Ma, with large populations around

this same age (n = 23) and 291 Ma (n = 45). The relative probability plot shows high peaks at 67 Ma (Maastrichtian) and 291 Ma (Sakmarian).

Sample SP3-92 (Pajarito Member, Purilactis Fm.)

The maximum depositional age obtained for this sample is 69.3±0.8 Ma (Figure 11c), with large populations at 73 Ma (n = 37, Late Cretaceous), 292 Ma (n = 15, Early Permian), 304 Ma (n = 12, Late Carboniferous), and 204 Ma (n = 8, Late Triassic). Its highest relative probability peaks are found at 73 Ma (Campanian), 204 Ma (Rhetian) and 292 Ma (Sakmarian).

Sample SP3-94 (Vizcachita Member, Purilactis Fm.)

The second sample of the Vizcachita Member, found towards its base, shows some noteworthy differences (Figure 11d). The maximum depositional age for this sample is 65.2±0.7 Ma, around which it has its largest population (n = 47 for 69 Ma, Late Cretaceous). A smaller population is also found at 76 Ma (n = 7), and only n = 3 zircons at 297 Ma (Early Permian). As with its composition, its relative probability plot differs from that of sample SP3-86, although it shares a peak at 69 Ma (Maastrichtian).

Population provenance

Many of the populations found in these samples have already been linked to their possible geological sources by Bascuñán et al. (2016). A summary of each identified source is shown below.

The oldest and most recurring population belongs to the 291-304 Ma range (early Permian-late Carboniferous), which has been ascribed to the upper Carboniferous-Permian units cropping out along the Cordillera de Domeyko, such as the Complejo Intrusivo Sierra de Limón Verde (Marinovic and Lahsen, 1984), the Agua Dulce Formation, and other granitoids and related intrusives (Basso and Mpodozis, 2012; Breitkreuz et al., 1992; Ramírez and Gardeweg, 1982). Only one of the samples shows a sizeable population belonging to the Late Triassic (204 Ma), whose provenance might be one of several Triassic outcrops, such as the Las Lomas and El Bordo beds

(Figure 2, Basso and Mpodozis, 2012), or the uppermost Tuina Formation (Henríquez et al., 2014; Narea et al., 2015). The detrital zircons associated with the Late Jurassic-Early Cretaceous (142 Ma) derive from the erosion of of andesites and intrusives within the age range located farther to the west, around the Coastal Cordillera (Oliveros et al., 2006; Pichowiak et al., 1990). The basal units of the Tonel Formation could also be a source of recycled zircons (Bascuñán et al., 2016).

The populations within the Late Cretaceous show different clusters, of which some are closer to the early Late Cretaceous (for example, Sample SP3-85). These may come either from formations representing the volcanic arc of that time in the Central Valley (Quebrada Mala and Paradero del Desierto formations; Cortés, 2000; Marinovic and García, 1999). Basso and Mpodozis (2012) also report intrusives with ages between 76-99 Ma intruding the Caracoles Group at the Cerro de Caracoles area. The latest Upper Cretaceous-Paleocene zircons, which reach into the Danian, may come from the erosion of various intrusives of Late Cretaceous-Paleocene age west of the study area, of which the closest outcrops can be found around Cerro Quimal, southwest of the study area (Basso and Mpodozis, 2012; Mpodozis et al., 2005).

5.-Discussion

The results obtained above and their integration (Figure 12) aid in understanding the evolution of the Salar de Atacama Basin, and of the Pre Andean Depression. The gravimetric modeling of the Barros Arana Syncline coincides with the interpretation of the syncline as obtained from seismic sections (Figures 4 & 6), although, and in contrast with previous interpretations, the presence of Late Cretaceous-Paleogene units has been identified both to the west and east of the syncline. To the west, these units are part of the first gravimetric low, and are overlain by the outcropping Tuina Formation (Figure 2). This area, comprising most of the western flank of the syncline, consistently shows the highest interval velocities within the study area regardless of depth, also showing large vertical gradients when compared with areas farther to the east (Figures 8 & 9). The reason for this segmentation of the velocity properties within the study area can be ascribed to the presence

beneath the surface of both the Tuina Formation and the formations comprising the syncline, which are expected to possess higher velocities than their more recent counterparts, based on lithology alone. The presence of Late Cretaceous-Paleocene intrusives (Figure 2) may also affect the velocity around this area, but their outcrops are scarce and widely spaced, and, as such, their effect on the measurements may be only local; the same argument can be made for the gravity modeling. The decrease in velocity seen in the eastern flank of the syncline/western side of the basin, at all depth slices (Figure 8), must take into consideration the lack of velocity data around this area, with a gap in velocity points roughly between the syncline axis and the western border of the Llano de la Paciencia. An analysis of the points north of this area (Figures 2, 8 & 9b) shows that the transition from the syncline towards the basin might be smoother than seen in the velocity cross-section (Figure 9a), with a steady drop in velocity and a trend semi parallel to the topography. This transition agrees with the structural continuity seen in the seismic sections due south (Figures 6 & 7), where the basement is progressively found at an increasing depth towards the east. Some variations may occur due to the position of the Oligo-Miocene Tambores Formation, which have been modeled in the gravity section as less dense than their older counterparts, and whose thickest deposits are found near the center of the eastern flank of the syncline (Figure 2). However, the gravimetric/velocity sections are located on the southern, thinner parts of this formation, which should only affect measurements mildly (see above).

The velocity and gravity models do not allow for the differentiation between the members belonging to the Tonel, Purilactis and Barros Arana Formations (Purilactis Group *sensu* Mpodozis et al., 2005), but they can be clearly distinguished from the outcropping Oligo-Miocene or recent strata (Figure 5b), which is relevant to infer the presence of the former units beneath the surface to the east. In particular, the low-density San Pedro Formation, which comprises most of the Cordillera de la Sal, is the most sensitive to variations in thickness and shape regarding the gravimetric model, and thus delimits the late Paleogene-Neogene geometry of the basin. Regarding

its shape, the gravimetric model shows a steady drop in gravity from the syncline border towards the Cordillera de la Sal, where the gravity signal suggests a depocenter with a higher slope on its west-tilted eastern edge (Figure 10). This feature may be due to the proximity to the surface of Triassic units, which is obtained both from the modeling and the analysis of seismic sections, and also because of the pop-up like deformation of the Late Cretaceous-Paleocene rocks assumed to underlie the San Pedro Formation (Figures 7 & 10). The bottom, scoop-shaped surface of the San Pedro Formation shows an increasing depth northward, from around 800 m in Figure 7 to 1200-1300 m in Figure 6, which is consistent with the gravity modelling. As for the velocities within this depocenter, they are on average lower than those found, at the same altitude in the syncline area, and the slices between 1500 and 1250 m a.s.l. show a local, roughly NNE, high-velocity zone beneath the Cordillera de la Sal, which might be related to the proximity of Triassic and Upper Cretaceous-Paleocene units, albeit not conclusively (Figure 8). The cross section in this area presents artifacts or noise possibly arising from the intense deformation of the Cordillera de la Sal, which also includes salt diapirs and other complex structures arising from salt tectonics (Figure 2; Rubilar et al., 2017; Wilkes and Görler, 1994). A different situation can be observed east of the Cordillera de la Sal, where the velocity cross-section shows a prominent, near-horizontal contrast between low-velocity units above (up to 2600-2800 m/s), and high-velocity units below (Figures 8 and 9). This abrupt transition is at an altitude between 1400-1600 m a.s.l., which is consistent with the limit between the San Pedro Formation and older Upper Cretaceous-Paleogene units as interpreted from the seismic sections (Figure 7). Accordingly, this limit was used to constrain the gravimetric modelling of the low-density deposits, underscoring again the contrast between the San Pedro Formation and the pre-Oligocene units, as described to the west.

The addition of new U-Pb detrital zircon age data is relevant to further unravel the development of the Salar de Atacama Basin. The obtained age populations are in general agreement with those previously published by several authors (see Table 1), with minor differences. As such, the

populations identified in these rocks indicate the erosion of a source composed mainly of Late Cretaceous and Permian-Carboniferous rocks, with minor additions of Late Jurassic-Early Cretaceous and Late Triassic zircons. The sources of these zircon populations have been shown to lie west of the study area, which is also supported by previous paleocurrent studies (Bascuñán et al., 2016; Hartley et al., 1992a, 1988). This western, exhumed source might range from the Cordillera de Domeyko to sources even farther to the west, such as the Late Cretaceous rocks of the Central Valley and the Late Jurassic-Early Cretaceous arc of the actual Coastal Cordillera, in successive steps (Bascuñán et al., 2016).

What is strikingly different from previous data is the recognition of younger zircon populations in the Purilactis Formation reaching the Danian (earliest Paleocene) (Figure 11b, d). They are particularly evident in the Vizcachita Member, whose maximum depositional ages are clearly from the K-T interval, thus redefining the age of the Purilactis and Barros Arana Formations, which were previously assigned to the Late Cretaceous-KT range (107-65 Ma, e.g., Arriagada et al., 2006a; Bascuñán et al., 2016; Jordan et al., 2007), and whose cap was presumed to be the volcanic Cerro Totola Formation found south of the study area, with ages between 61-70 Ma (Table 1; Basso and Mpodozis, 2012; Mpodozis et al., 2005). Also, the age of the Vizcachita Member is in partial agreement with the Ar-Ar age of an altered lava flow within the same member obtained by Flint et al. (1989), dated at 63.8±1.9 Ma. As such, the Vizcachita Member is a time equivalent of the Cerro Totola Formation, which is seen overlying lower members of the Purilactis Formation to the south, and which has numerous age-related intrusives around Cerro Quimal and within the Tonel-lower Purilactis Formation (Andriessen and Reutter, 1994; Arriagada, 1999; Basso and Mpodozis, 2012; Mpodozis et al., 2005).

The question of the age of the remaining units within the Barros Arana Syncline is relevant to address the tectonic history of the basin. The only visible geological relation between the Barros Arana Formation and younger units is its angular unconformity with the Oligo-Miocene Tambores

Formation (Figures 2 & 6), which could make these units fit a time range similar as that proposed by Charrier and Reutter (1994), reaching well into the Paleogene. This also brings into discussion the temporal relationship between these units and the Loma Amarilla and Naranja Formations, the latter of which is found south of the study area, but which has been considered part of the Paleocene evolution of the basin (Figures 2, 3 & 4; Arriagada et al., 2006a; Jordan et al., 2007; Mpodozis et al., 2005; Pananont et al., 2004). Reiners et al. (2015), based on U-Pb and (U-Th/He) dating of single zircon crystals, obtained ages ranging from 49-308 Ma for the Loma Amarilla Formation and 72-81 Ma for the Naranja Formation (Table 1), making their youngest zircons older than previously published depositional ages (between 35-45 Ma and 58-45 Ma, respectively, following Hammerschmidt et al. (1992) and Mpodozis et al. (2005)). It must be noted that the maximum depositional ages for the Naranja Formation were obtained 70 km south of Cerro Quimal (Gardeweg et al., 1994; Solari et al., 2017), and as such, the ages of Reiners et al. (2015) are the closest ones for this formation within the study area. For this study, it has been considered that the upper Purilactis-Barros Arana Formations may be partial equivalents to the Naranja Formation (Figure 4), which raises questions regarding both the angular unconformities described to the south along the El Bordo Escarpment, and those assumed for the units within the basin as correlated with seismic sections (Arriagada, 1999; Arriagada et al., 2006a; Jordan et al., 2007; Mpodozis et al., 2005; Muñoz et al., 2002; Pananont et al., 2004). Another option, which is in partial agreement with previous stratigraphic models, is to place these units within a narrow time range (65-58 Ma). This issue may be resolved with the addition of geochronological data from scarcely dated units, but, in any case, the units belonging to the syncline were deposited under compressive conditions associated with the development of a foreland basin during the Late Cretaceous (Arriagada et al., 2006a; Bascuñán et al., 2016), which continued during the Paleogene (including the K-T Event described by Cornejo et al. (2003, 1993)). These deposits would have been then folded and deformed during the Eocene-Oligocene Incaic Event, a widespread deformation event with high exhumation rates around the Cordillera de Domeyko, clockwise tectonic rotations south of the Arica

Bend and the formation of the Bolivian Orocline (Arriagada et al., 2008, 2006a, 2006b; del Papa et al., 2010; Maksaev and Zentilli, 1999; McQuarrie, 2002; Narea et al., 2015; O'Driscoll et al., 2012). Regarding the presence of the Loma Amarilla Formation within the basin, it cannot be either confirmed or overruled with the data presented; it may well form thin intervals, as proposed by Pananont et al. (2004), owing to the strong exhumation and deformation during the time of their deposition, or they may have been cannibalized shortly after their deposition. Both alternatives are in agreement with the deposition of the Loma Amarilla in a wedge-top depozone (DeCelles and Giles, 1996).

After the Incaic Event, extensional conditions, together with strike-slip tectonics, have been inferred for the late Oligocene-early Miocene within the basin (Jordan et al., 2007; Pananont et al., 2004; Rubilar et al., 2017). One of the structures attributed to have generated extension during this stage corresponds to the Paciencia Fault (*sensu* Pananont et al. (2004)). This fault, found at the eastern flank of the Barros Arana Syncline, would have generated around 6±1 km of vertical displacement, effectively controlling the deposition of the Tambores and San Pedro formations. Arriagada et al. (2006a) found no conclusive evidence for this fault at the surface, but Jordan et al. (2007) and Henríquez et al. (2014) document small normal faults affecting Oligocene-Miocene gravels around the Llano de la Paciencia Area (Figure 2). Also, Martínez et al. (2017) reported mainly inverted and contractional structures in the Salar de Punta Negra Basin, which corresponds to the southward prolongation of the Salar de Atacama.

The geophysical and seismic data compiled and analyzed in this study agree more closely with a contractional setting for most of the basin history (Figure 12). Under this scheme, sedimentation in the basin would have started during the Peruvian Phase (Bascuñán et al., 2016), and continued throughout the Paleocene. The actual structural configuration of the basin would have been established mainly during the Incaic Event, with the folding and clockwise rotation of Mesozoic-Cenozoic deposits, and the establishment of a thick-skin, east-verging reverse fault system. Some of

these faults would have then been reactivated during the late Miocene (Quechua-Pehuenche events; (Charrier et al., 2007; Salfity and Marquillas, 1994; Yrigoyen, 1993), leading to the present structure of the basin, especially around the Cordillera de la Sal area and the western flank of the Barros Arana Syncline. The contribution of strike-slip tectonics cannot be assessed with the methods provided in this contribution.

A compressive, though somewhat stalled setting for the Oligocene-early Miocene is consistent with diverse findings in the Central Andes of NW Argentina and southern Bolivia (Allmendinger et al., 1997; Carrapa et al., 2012; Carrapa and DeCelles, 2008, 2015; Decelles et al., 2011; DeCelles et al., 2015; Del Papa et al., 2013; Horton, 1998; McQuarrie, 2002; Quade et al., 2015; Siks and Horton, 2011), showing a gradual shift of the migration front within the Eastern Cordillera and the rising of the eastern margin of the Puna Plateau. Compressive conditions have also been documented north of the study area in Chile, where Charrier et al. (2013) show no significant extensional event for the Precordillera and Western Altiplano between 18°-19°S. Instead, the tectonostratigraphic evolution of the area is more consistent with the development of a retroarc foreland basin in the Altiplano area during the late Eocene-Oligocene, and the development of the West- and East-verging Thrust Systems during the late Oligocene-early Miocene. The first system generated a significant amount of uplift (0.1 mm/yr) at the western side of the Altiplano, between 26-8 Ma (Farías et al., 2005; Nester and Jordan, 2012). Also, Martínez et al. (2017) proposed a synorogenic character for the Pampas de Mula Formation in the Salar de Punta Negra Basin, immediately south of the Salar de Atacama.

Finally, the analysis above suggests that the Salar de Atacama Basin was receiving sediments from western sources related to the progressive shift eastwards of the migration front from the Late Cretaceous onwards, which continued well beyond the Paleocene (Vizcachita Member-Barros Arana Formation). After the rapid shift of the deformation front away from the basin into the Eastern Cordillera (Carrapa and DeCelles, 2015), the basin, now in a hinterland position, would

have started accumulating deposits of the Paciencia Group, with coarser units closer to more elevated areas (Tambores Formation), and around 800-1200 m of finer units within the actual basin (San Pedro Formation). After the Oligocene magmatic lull, several large ignimbrites were deposited around the basin, and the current magmatic arc was established shortly afterwards (Charrier et al., 2009; Kay and Coira, 2009). Further compression, rotation and reactivation of previous structures would have then occurred within the basin (Cordillera de la Sal), and at the flanks of the Barros Arana Syncline (Figure 2; Arriagada et al., 2006a; Hartley et al., 1992b; Mpodozis et al., 2005; Rubilar et al., 2017).

6.-Summary and Conclusions

A review of the geology of the Salar de Atacama area, and the addition of independent geophysical and geochronological constraints, leads to a deeper understanding of the geological evolution of the basin during the late Mesozoic-Cenozoic. Seismic velocities within and around the basin show a segmentation of its physical properties, roughly corresponding to the boundaries of different geological units. The seismic reflection profiles show that the structure at this latitude consists of an east-verging thrust system, mainly involving Permo-Triassic, Upper Cretaceous and Paleogene (?) units. The gravimetric survey shows that the main density contrast corresponds to the limit between the evaporitic and clastic units of the San Pedro Formation, the deposits of the Purilactis Group and the presence of Triassic outcrops. The San Pedro Formation shows a stratigraphic wedge whose thickness increases eastwards, and clear angular unconformities separate it from previous units. The U-Pb data show populations in general agreement with previous studies, although a prominent late Campanian-early Maastrichtian signal appears. The stratigraphic continuity of the units within the syncline, and their strongly unconformable relation to the overlying Oligocene deposits, show that the structural configuration of the area was primarily formed during the late Eocene-early Oligocene Incaic Event. The late Oligocene deposits would represent a post-orogenic infill after the eastward migration of the orogenic front, with varying amounts of compression. This compression

would have been more relevant during the late Miocene, which shows a reactivation of previous reverse faults and the generation of the Cordillera de la Sal. This relatively continuous, compressive history of the basin throughout the Cenozoic is in general agreement with regional studies both in Chile and in other neighboring areas of the Central Andes.

7.-Acknowledgements

We would like to thank Empresa Nacional del Petróleo (ENAP) for the access to the seismic sections of the Basin. We are also deeply grateful to Alvaro Henríquez and Andrés Fock of Sociedad Química y Minera de Chile S.A. (SQM) for their logistic support and access to the Toconao camp. We thank the IRD-GET for providing the CG-3 Scintrex gravimeter and Midland Valley Ltd., for the license for MOVE 2017. S.B. acknowledges the support of CONICYT-Chile (Grant 21150380). A.M. acknowledges the support of CONICYT-Chile, under the grants FONDECYT Nº 3150160 and PIA/Anillo ACT17202. We also appreciate the suggestions and corrections by two anonymous reviewers, which improved this contribution. Sergio Villagrán, Marco Vaccaris and Luis Acevedo are deeply thanked as well for their invaluable field support and software assistance.

8.-References

Al-Chalabi, M., Rosenkranz, P.L., 2002. Velocity-depth and time-depth relationships for a decompacted uplifted unit. Geophys. Prospect. 50, 661–664. https://doi.org/10.1046/j.1365-2478.2002.00345.x

Allmendinger, R.W., Jordan, T.E., Kay, S.M., Isacks, B.L., 1997. The Evolution of the Altiplano-Puna Plateau of the Central Andes. Annu. Rev. Earth Planet. Sci. 25, 139–174. https://doi.org/10.1146/annurev.earth.25.1.139

Amilibia, M., Sàbat, F., McClay, K.R., Muñoz, J.A., Roca, E., Chong, G., 2008. The role of